



# Experimental Study on the Performance of FRP Grid Reinforced ECC Composite Layer-Concrete Interface

Weiwen Li<sup>1</sup>, Jie Liu<sup>1</sup>, Jiahao Zhang<sup>1</sup>, Shiyang Tang<sup>1</sup>, Meizhong Wu<sup>1</sup>,  
and Xu Yang<sup>2</sup>(✉)

<sup>1</sup> Guangdong Provincial Key Laboratory of Durability for Marine Civil Engineering, College of Civil and Transportation Engineering, Shenzhen University, Shenzhen 518060, China

<sup>2</sup> College of Civil and Environmental Engineering, Harbin Institute of Technology, Shenzhen 518055, China  
ydyn12021@yeah.net

**Abstract.** In this paper, the bond slip between the composite reinforcement layer and concrete is studied by single shear test. The composite reinforcement layer contains the CFRP (Carbon Fiber Reinforced Polymer) grid embedded within ECC (Engineering cementitious composites) matrix. Considering the influence of bond length, matrix type and ECC strength, the failure mode of the interface and the effect of various factors are clarified through the discussion of the experimental phenomenon, load slip relationship and bond slip relationship. The result indicated that the effective bond length increases with the decrease of ECC matrix strength, when the effective bond length exceeds 550 mm or the ECC matrix strength is greater than E40, the failure load can be increased. In comparison with mortar composite layer, ECC composite layer tends to be relatively ductile. Finally, two of existing FRP-concrete interface models were selected to fit the experimental curve, and the fitting effect of existing FRP-concrete interface models is acceptable.

**Keywords:** Interface · ECC · FRP · Concrete · Bond behavior · Single shear test

## 1 Introduction

As a kind of material for reinforcement, carbon fiber reinforced polymer (CFRP) has a lots of advantages, such as light weight, high strength, and corrosion resistance. Nevertheless, what can't be ignored is the disadvantage of its poor bonding performance with concrete. So many researchers use inorganic cement-based materials to replace epoxy resin, which is commonly used as a binder for FRP. Therefore, many studies on the FRP-concrete interface using inorganic cementitious materials as binders have begun to emerge, among which fabric-reinforced cementitious matrix (FRCM), textile-reinforced mortar (TRM) [1–3] and other reinforcements have emerged. This research direction produced a lots of achievement, including the interface of FRP strip-concrete [4], the interface of FRP woven mesh-concrete [5], etc. However, these materials tend to have

low stiffness and poor bonding performance, which leads to unsatisfactory reinforcement effects on the structure.

A lot of researches have shown that CFRP grid has the characteristics of high rigidity and good stability, and has obvious advantages in the reinforcement of concrete structures [6]. At the same time, engineering cementitious composites (ECC) have the advantages of multiple cracks and strong adhesion to concrete [7–9]. According to the above summary, we can know that the composite layer formed by the CFRP grid embedded with ECC matrix (ECC composite layer) can provide a new idea for the reinforcement of structures in engineering.

Therefore, this paper researched the bonding performance of the interface between ECC composite layer and concrete. The failure form and failure load are discussed firstly, and then the load-slip curve and bond-slip curve are analyzed, the experimental parameters including the bond length and the types of matrix as well as the strength of ECC matrix. Finally, the constitutive model of the interface between FRP and concrete was used to fit the experimental bond-slip curve. The results show that the model used in this paper is great, and provides a good empirical theory and research direction for the subsequent study of the bond performance of the ECC composite layer-concrete interface.

## 2 Experimental Study

In this single shear test, the composite layer, bonded on the concrete block, as shown in Fig. 1. A total of 20 specimens were tested, and the research variables are shown in Table 1.

### 2.1 Materials

The average cube strength and elastic modulus of the concrete is 25.5 MPa, 26.8 GPa. The average cube strength of mortar is 34.5 MPa, which is close to ECC within 60%

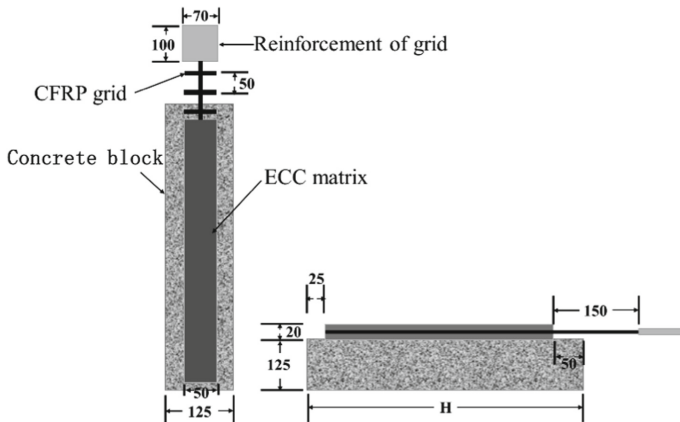


Fig. 1. Specimen dimension (units: mm).

fly ash. And configure ECC with different strengths by adjusting the content of fly ash [10], the details of ECC (unit in g/L) are listed in Table 2 as follows [11].

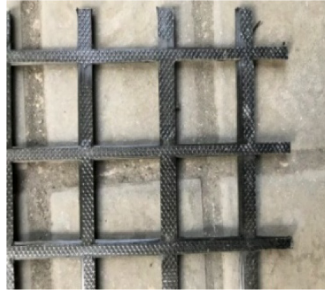


Fig. 2. CFRP grid.

The size of the CFRP grid is 50 mm × 50 mm, and the cross-sectional area of a single grid is 26.4 mm<sup>2</sup> (See in Fig. 2). The test results show that the tensile strength of the CFRP grid is 1515 MPa and the elastic modulus is 114.8 GPa.

### 2.2 Specimen Preparation

The dimensions of each part of the test specimens are shown in Fig. 1. The layout of the strain gauge can be seen from Fig. 3. It should be note that the pouring sequence is to place a layer of 10 mm thick matrix firstly, and them the grid is placed on the surface of the matrix, finally a layer of 10 mm thick matrix is covered.

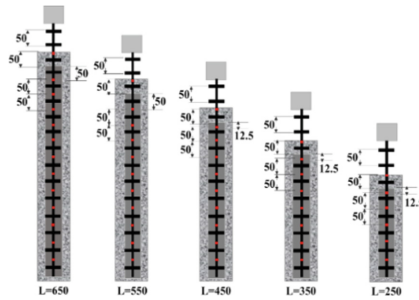
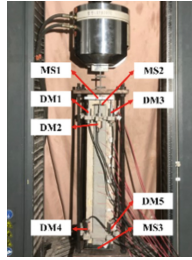


Fig. 3. Details of strain gauge (units: mm).

### 2.3 Test Methods

This single shear test adopts displacement-controlled loading, and the loading rate is 0.2 mm/min. As shown in Fig. 4. The machine applied load to the composite layer by clamping the end reinforcement sheet of grid. Paste three metal sheets (MS) and 5 displacement meters (DM) are used to measure the displacement, and several strain gauges (SG) can collect data of strain of grid.



**Fig. 4.** Schematic of single shear test.

**Table 1.** Details of characterizations of specimens.

Specimens	Matrix types	Bond length (mm)	Numbers of specimens
M-250	Mortar	250	5
M-350		350	
M-450		450	
M-550		550	
M-650		650	
E40-250	ECC containing 40% FA	250	5
E40-350		350	
E40-450		450	
E40-550		550	
E40-650		650	
E60-250	ECC containing 60% FA	250	5
E60-350		350	
E60-450		450	
E60-550		550	
E60-650		650	
E80-250	ECC containing 80% FA	250	5
E80-350		350	
E80-450		450	
E80-550		550	
E60-650		650	

**Table 2.** Mixture proportions and properties of ECC.

Types	Cement	Quartz sand	Fly ash	Water	Water reducer	PE fiber	Ultimate compressive strength/MPa	Ultimate tensile strength/MPa
E40	800	266.6	533.3	400	5	15	51.5	6.489
E60	533.3	266.6	800	400	6	15	34.9	5.821
E80	266.6	266.6	1066.6	400	7.5	15	22.1	2.878

### 3 Result

#### 3.1 Failure Mode

The test results show that, regardless of ECC composite layer or the mortar composite layer, most of the failure modes of the specimens show the interfacial debonding (DB), and only the failure mode of specimen E80-650 shows grid fracture and interface is not debonded (FGB).

By comparison, the mortar composite layer is brittle failure and irregular to follow, while the ECC composite layer is relatively ductile and its debonding process shows two different forms of sudden peeling and gradual debonding as the bond length increases. The load-slip curve is shown in Fig. 6. In a word, sudden peeling mainly occurs in the

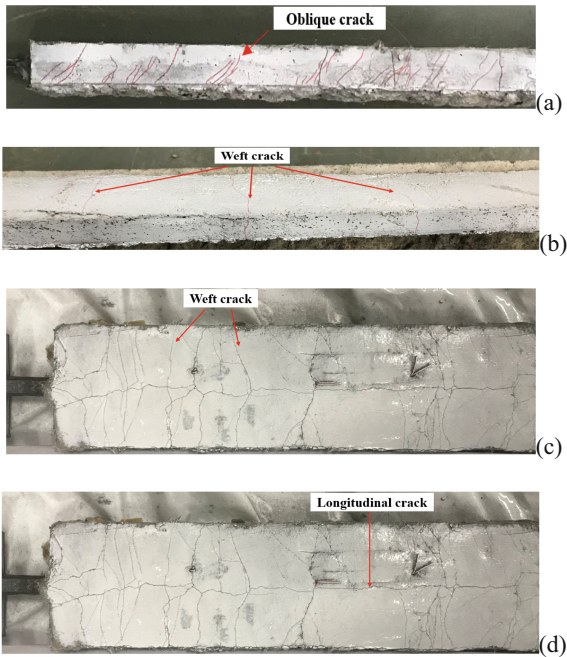


**Fig. 5.** Details of cracks (a, b and c are for ECC, d is for mortar).

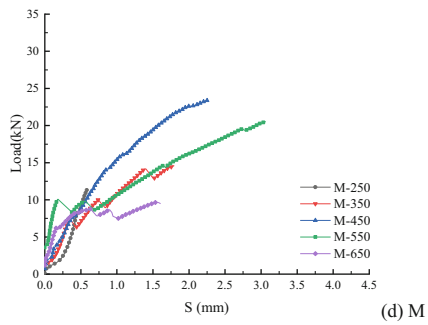
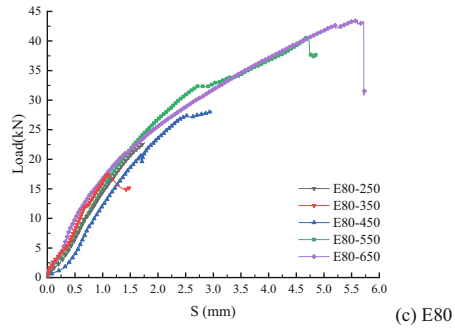
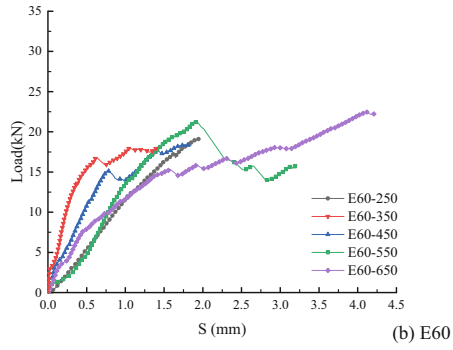
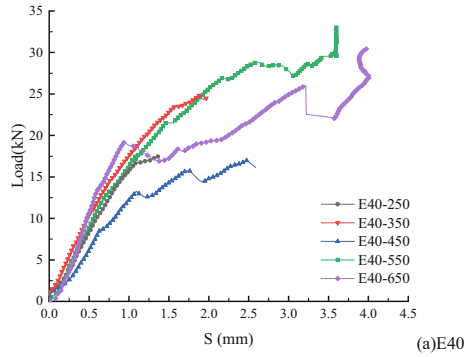


**Fig. 6.** Load-slip curve of specimens.

specimens with bond lengths of 250 mm and 350 mm. There are only a few cracks before the specimens are destroyed, and finally the interface suddenly deboned. Nevertheless, gradually debonding occurs in the specimens with bond lengths of 450 mm, 550 mm, and 650 mm. Its failure characteristics are mainly termed (1) the specimen is in the elastic stage and there is no obvious damage when the load is small in the early stage of the test; (2) As the load increases to larger, the upper surface of the composite layer loading end began to bring fine cracks (weft cracks) into being, which are perpendicular to the loading direction; (3) When the load continued to increase in the middle of the test, the longitudinal cracks will appear, the number of cracks gradually increases and develops toward the free end, and the composite layer peels off at the loading end partially so that the amount of interface slip increases; (4) In the latest stage, The width and number of cracks in the composite layer further expand and become stable. The range of local debonding extends to the free end, and the amount of interface slip is about to reach its peak. Finally, the entire composite layer is completely peeled and destroyed. Cracks can be seen in Fig. 5.

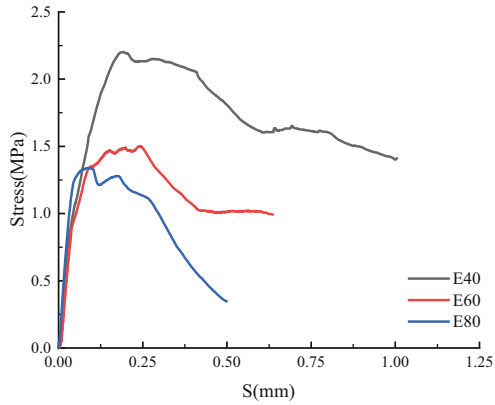
### 3.2 Failure Load

The failure load of each specimen is summarized in Table 3, and the influence of factors such as the bond length, the strength of ECC matrix and the type of matrix are discussed.

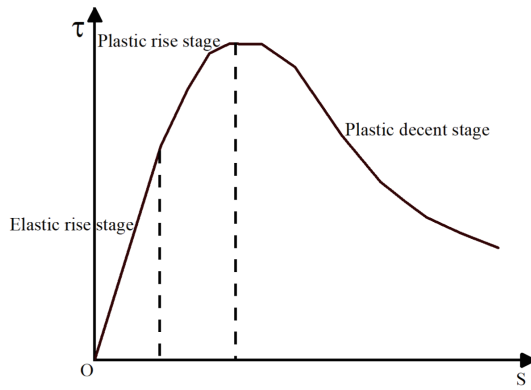
In view of the effect of bonding length, the failure load increases with the bond length of the composite layer increases. When the bond length of the composite layer exceeds the effective bond length, the failure load will not continue increase. Therefore, the effective bond range of different matrix composite layers can be roughly determined. The effective bond length ranges of E40 and E60 specimens is 550 mm–650 mm, and the effective bonding length of E80 specimens is greater than 650 mm, as is shown in Table 3. Among them, the composite layer of the matrix of E40, E60 and Mortar showed many decreases after the bond length exceeded 550 mm. The author believes that this is mainly due to the inevitable shrinkage cracks formed during curing [12].

When the strength of ECC matrix is different, it is found that the interface failure load does not change linearly with the decrease in the strength of the ECC matrix when the bond length exceeds 450 mm. In general, the greater strength of the ECC matrix results in the greater ultimate bond stress of the interface, so that the interface failure load will also increase. However, the test results show that the failure load of E60 group of specimens has decreased, while the failure load of E80 group of specimens has increased significantly. The reason is that the effective bond length of E80 specimens is affected by the strength of the ECC matrix, and it also can be said that the smaller the strength of ECC matrix, the longer effective bond length. So under the coupling effect of the maximum bond stress of interface and the effective bond length, the failure load of E80 specimens increased.

The type of matrix is different, and the bonding performance is also different. As shown in Table 3, the failure load and the slip of ECC composite layer are significantly greater than that of the mortar composite layer. It can be seen that ECC composite layer matrix has significant advantages of high ductility and large bearing capacity of interface.



(a) Bond-slip curve of E40, E60 and E80



(b) Each stage of bond-slip curve

**Fig. 7.** Bond-slip curve.

**Table 3.** Test result.

Specimens	Global slip/mm	Failure load/kN	Failure mode	Prediction of effective bond length
E40-250	1.24	17.4	DB	550 mm–650 mm
E40-350	1.78	24.8	DB	
E40-450	2.46	17.0	DB	
E40-550	3.37	33.0	DB	
E40-650	3.99	30.5	DB	
E60-250	1.79	19.1	DB	550 mm–650 mm

(continued)



**Table 3.** (continued)

Specimens	Global slip/mm	Failure load/kN	Failure mode	Prediction of effective bond length
E60-350	1.27	18.1	DB	
E60-450	2.43	18.4	DB	
E60-550	3.09	21.19	DB	
E60-650	4.03	22.5	DB	
E80-250	1.59	22.8	DB	≥650 mm
E80-350	1.36	17.4	DB	
E80-450	2.7	28.1	DB	
E80-550	4.5	40.7	DB	
E80-650	5.5	43.3	FGB	
M-250	0.5	11.4	DB	450 mm–550 mm
M-350	1.7	14.6	DB	
M-450	2.2	23.3	DB	
M-550	3.0	20.5	DB	
M-650	3.5	17.5	DB	

### 3.3 Bond-Slip Curve

According to the results, the displacement value of the composite reinforcement layer at the free end is almost zero, so it can be ignored. The value of the strain gauge is calculated by differential interpolation to obtain the bond-slip curve. According to the shape of the curves, the bond-slip curves of E40, E60, and E80 specimens can be divided into three stages: elastic rising stage, plastic rise stage, and plastic fall stage, as shown in Fig. 7. Among them, the elastic rise stage curve is roughly linear, the bond stress of interfacial increases rapidly with the increase of slip, and the bonding stiffness of the interface is larger; The interface shear stress of the plastic rise stage is greater than the chemical bonding force between concrete and ECC, the growth rate of interface shear stress decreases gradually with the increase of slip, and the bonding stiffness of the interface gradually becomes smaller; When the shear stress peak is reached, the curve enters the plastic fall stage. At this time, the interface is damaged, it is also means that the aggregate on the interface between ECC and concrete wears, the shear stress of the interface decreases and the amount of slippage increases rapidly. The overall shape of the bond slip curve, meanwhile, is not affected by the strength of the ECC matrix, and before the composite layer is completely peeled off, a residual stress section similar to the FRCM bond slip curve appears at the end of the bond slip curve [4] This is mainly due to the mechanical occlusion of the ECC and concrete interface and the bridging effect of the fibers at the ECC matrix interface, and the bond-slip curve shows a certain degree of ductility.

### 3.4 Comparison of Models

Considering that there are few studies on prediction models related to the interface between ECC and concrete, but the prediction models related to the interface between FRP and concrete have a wide range of applications. Among them, the models proposed by He [13] and Wu [14] have great prediction effects, as seen Eq. 1 and Eq. 2. These two models are fitted to the experimental results, and the fitted bond-slip curve is consistent with the experimental results, as shown in Fig. 8. In the rising section of the curve, both the He model and the Wu model are in good agreement with the experimental values; In the falling section, the experimental data are basically distributed on both sides of the fitting curve of Wu model, while the fitting curve of He model has relatively poor accuracy. Table 4 lists the relevant fitting parameters and the fitting coefficients of each model. The average values of the fitting coefficients R2 of He model and Wu model are 0.818 and 0.965, respectively. It can be seen that using Wu model as the constitutive

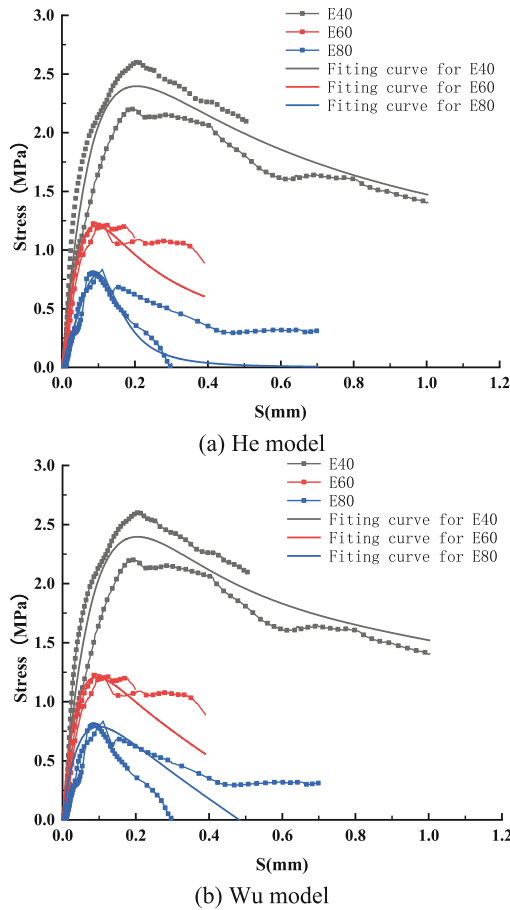


Fig. 8. Fitting curve of bond-slip relationship.

model of bond-slip relationship between the ECC composite layer and concrete will be more accurate.

He model:

$$\tau(s) = \tau_{max} \frac{s}{s_0} \left( \frac{n}{(n-1) + (s/s_0)^n} \right) \quad (1)$$

Wu model:

$$\tau(s) = \frac{\tau_{max}(\omega + e^\omega - 1)}{(1 - e^{-\omega})^2(\omega + Ce^\omega + 1)} \left[ e^{-\frac{\omega s}{s_0}} + C - \frac{C + 2e^{-\omega} - 1}{\omega + e^\omega - 1} \cdot \frac{\omega s}{s_0} \right] \times \left[ 1 - e^{-\frac{\omega s}{s_0}} \right] \quad (2)$$

where  $n$  is a parameter that mainly controls the softening branch;  $\omega$  and  $C$  are infinite constants;  $\tau_{max}$  is the average maximum bond stress;  $s_0$  are the slip at the maximum bond stress.

**Table 4.** Fitting result.

Specimens	$\bar{\tau}_{max}/\text{MPa}$	$s_0/\text{mm}$	$n$	$R^2(\text{He model})$	$C$	$\omega$	$R^2(\text{Zhou model})$
E40-250	2.1	0.33	1.701	0.945	1.152	0.441	0.983
E40-450	2.39	0.21	1.412	0.976	1.135	0.384	0.993
E40-550	2.78	0.27	1.575	0.767	1.103	0.362	0.954
E60-250	1.26	0.13	1.453	0.836	1.155	0.650	0.923
E60-350	1.21	0.10	1.386	0.917	1.198	0.681	0.995
E60-450	1.74	0.11	1.539	0.680	1.155	0.639	0.945
E80-350	0.80	0.10	2.955	0.933	1.112	0.944	0.995
E80-450	0.93	0.31	1.219	0.377	1.115	0.962	0.906
E80-550	1.10	0.12	2.166	0.938	1.303	0.874	0.994
Average value				0.818			0.965

## 4 Summary

In this study, the bonding behavior of the interface between the FRP grid-reinforced ECC composite layer and concrete was studied by single shear test. The conclusions are as follows:

- (1) The debonding process of the interface between ECC composite layer and concrete is mainly divided into sudden peeling and gradual debonding as the bond length increases. Furthermore, the surface crack morphology of the ECC composite layer at the time of failure is not affected by factors such as the strength of ECC matrix, the types of ECC matrix, and the bond length.

- (2) The failure load of the interface between ECC composite layer and concrete is affected by the coupling of the effective bond length and the strength of ECC matrix. Under the condition that the effective bond length increases with the decrease of ECC matrix strength, when the effective bond length exceeds 550 mm or the ECC matrix strength is greater than E40, the failure load can be increased;
- (3) The test results show that the bond-slip curve of the interface between the FRP grid-ECC composite layer and the concrete is basically the same. It can be divided into three stages: elastic rising stage, plastic rising stage, and plastic falling stage. And fitting it with the bond-slip model of the interface between FRP and concrete can get a good fitting work.

**Acknowledgment.** The authors would like to appreciate the financial support provided by the National Natural Science Foundation of China (NSFC Grant Numbers: 51878415, 51908373). Technical support is acknowledged from Guangdong Provincial Key Laboratory of Durability for Marine Civil Engineering (SZU), No. 2020B1212060074.

## References

1. Bournas, D.A., Lontou, P.V., Papanicolaou, C.G., Triantafillou, T.C.: Textile-reinforced mortar versus fiber-reinforced polymer confinement in reinforced concrete columns. *ACI Struct. J.* **104**(6), 740 (2007)
2. ACI Committee 549: Guide to design and construction of externally bonded fabric-reinforced cementitious matrix (FRCM) systems for repair and strengthening concrete and masonry structures (2013). ACI 549.4R-13
3. Focacci, F., D'Antino, T., Carloni, C.: The role of the fiber–matrix interfacial properties on the tensile behavior of FRCM coupons. *Constr. Build. Mater.* **265**, 120263 (2020)
4. Nelson, L.A., Al-Allaf, M., Weekes, L.: Analytical modelling of bond-slip failure between epoxy bonded FRP and concrete substrate. *Compos. Struct.* **251**, 112596 (2020)
5. Jiang, J., Jiang, C., Li, B., Feng, P.: Bond behavior of basalt textile meshes in ultra-high ductility cementitious composites. *Compos. B Eng.* **174**, 107022 (2019)
6. Liu, Z., Yue, Q., Li, R., Ding, Y.: FRP grid in civil engineering applications. In: *The 9th National Symposium on FRP application in Construction Engineering* (2015)
7. Li, V.C., Leung, C.K.Y.: Steady-state and multiple cracking of short random fiber composites. *J. Eng. Mech.* **118**(11), 2246–2264 (1992)
8. Yang, X., Gao, W.Y., Dai, J.G., Lu, Z.D., Yu, K.Q.: Flexural strengthening of RC beams with CFRP grid-reinforced ECC matrix. *Compos. Struct.* **189**, 9–26 (2018)
9. Zheng, Y.: Experiment and calculation method research on reinforced concrete (RC) beams strengthened with the composite of FRP grid and ECC. A dissertation submitted to Southeast University (2018)
10. Liu, C., Bi, Y., Hua, Y.: Mechanical properties of PVA-ECC with high volume fly ash and mechanin analysis of fly ash. *Bull. Chin. Ceram. Soc.* **36**(11), 3739–3744 (2017)
11. Fiber reinforced polymer composite grids for civil engineering. GB/T 36262—2018
12. Li, M., Li, V.C.: Behavior of ECC/concrete layered repair system under drying shrinkage conditions/Das Verhalten eines geschichteten Instandsetzungssystems aus ECC und Beton unter der Einwirkung von Trocknungsschwinden. *Restorat. Build. Monuments* **12**(2), 143–160 (2006)

13. He, W., Wang, X., Ding, L., Wu, Z.: Experimental study on bond behavior of interface between fiber-reinforced polymer grids and concrete substrate. *Compos. Struct.* **257**, 113164 (2021)
14. Zhou, Y.W., Wu, Y.F.: General model for constitutive relationships of concrete and its composite structures. *Compos. Struct.* **94**(2), 580–592 (2012)